PHYSICAL REVIEW B **78**, 121405(R) (2008)

Adsorbate cluster expansion for an arbitrary number of inequivalent sites

D. Lerch, O. Wieckhorst, L. Hammer, K. Heinz, and S. Müller*
Lehrstuhl für Festkörperphysik, Universität Erlangen-Nürnberg, Staudtstrasse 7, D-91058 Erlangen, Germany
(Received 18 July 2008; published 22 September 2008)

The detailed knowledge of a system's ground state is the most important prerequisite to understand its physical properties. We have extended the cluster-expansion formalism to apply it to adsorbate systems with an in-principle arbitrary number of adsorbate sites. The formalism will be applied to a system where a number of different adsorbate sites are occupied already at $T=0$ K, H on the Ir(100)-(5×1)-H surface. It will be shown that our predictions are in quantitative agreement with the experiment.

DOI: 10.1103/PhysRevB.78.121405 PACS number(s): 68.43.Fg, 61.05.jh, 64.60.De, 71.15.Mb

An adsorbate's coverage-dependent ground-state configuration contains information which is important for various fields of applications such as catalysis, corrosion or the initial stages of nucleation, and epitaxial growth. Unfortunately, especially when several inequivalent sites come into play, the configuration space in which these ground states need to be identified easily surpasses the number of configurations that can be calculated directly by an electronic structure theory such as density-functional theory (DFT). One possible way out of this dilemma provides the combination of DFT calculations with the cluster-expansion (CE) methodology. In this Rapid Communication, we present the successful application of the CE method for the adsorption of hydrogen on the so-called (5×1)-H-reconstructed Ir(100) surface,[1] a system with as many as twelve inequivalent adsorbate sites (Fig. 1). This hydrogen-induced phase consists of nearly defect-free monatomic iridium chains on an otherwise unreconstructed Ir(100) surface and forms a perfect template for the epitaxial growth of magnetic nanostructures.[2]

The idea of the cluster-expansion[3] method is to express the atomically relaxed energy $E(\sigma)$ of an arbitrary lattice configuration σ on a well-defined lattice as

$$E(\sigma) = N\sum_{F} D_F \bar{\Pi}_F(\sigma) J_F, \tag{1}$$

where N denotes the number of atoms on the lattice, D_F the number of figures per class F, $\bar{\Pi}_F(\sigma)$ structure-dependent factors (so-called correlation functions) of a given configuration, and J_F the effective cluster interactions (so-called effective cluster interactions (ECI), for details see, e.g., Ref. 4). In practice, the error involved in the method comes from the sum which has to be truncated at some point. The "art" of the method is therefore to develop and apply efficient tools to control this error, i.e., to ensure that it is smaller than the accuracy demanded for the problem of interest.[5] A first expansion to the case of a binary adsorption problem with one site available has been achieved by Sluiter and Kawazoe,[6] where an adsorbate system with three independent adsorption states for H on the C top site of a freestanding graphene sheet has been performed. Here, the CE is to be applied to a multisite adsorbate system, with *all* sites to be occupied independent of each other. Thus, the different energetics and hence different interactions resulting from inequivalent sites need to be considered. This results in a formulation of the CE where the figures F do not only have to be discriminated according to their geometric shape but also according to the sites they connect, which is equivalent to a *space dependency* $F(R)$,

$$E(\sigma) = N\sum_{F(R)} D_{F(R)} \bar{\Pi}_{F(R)}(\sigma) J_{F(R)}. \tag{2}$$

In the example of the Ir(100)-(5×1)-H surface, Fig. 1, the ECI for the nearest-neighbor pair interaction between, e.g., the connected sites B3 and B4 must differ from that between sites B3 and B2, even though these figures belong to the same geometric class F. This problem is comparable to the construction of layer-dependent interactions to treat segregation phenomena at alloy surfaces,[4,7,8] whereby the layers included in the CE now take the role of the different adsorbate sites in a CE for multisite-adsorption problems.

Although this ansatz is in principle applicable for an arbitrary number of inequivalent sites, in practice, there exists a limitation which has nothing to do with the CE itself, namely, the computing power available to obtain the *ab initio* input required for the determination of $J_{F(R)}$. Especially for the treatment of surface problems, this time factor becomes dominant due to the much higher number of atoms necessary to model surface structures via DFT compared to bulk structures. Therefore, first-step DFT calculations have to be performed in order to receive the heat of adsorption for the geometrically fully relaxed systems with only one hydrogen atom adsorbed on one of the 12 inequivalent high-symmetry

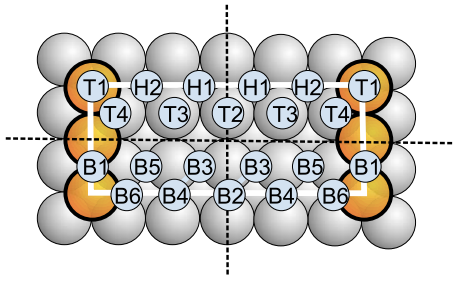

FIG. 1. (Color online) The 12 inequivalent adsorbates sites on Ir(100)-(5×1)-H surface (spheres with capitals) and their symmetric equivalences within the (5×1) unit cell (spheres with minuscules). The marked pair figures (B3-B4 and B3-B2) illustrate that they have to be treated independently because of the inequivalence of the sites B2 and B4.

adsorption sites (Fig. 1). It will be shown that, for the system under consideration, this allows for a determination of the number of sites, which is required in the CE to permit predictions over the complete range of coverages of interest. In a second step, the selection of adsorption geometries for arbitrary structures necessary to stabilize the CE Hamiltonian is controlled by a self-consistent loop, which is described in detail elsewhere.[8]

However, besides the configuration space of the adsorbates, the number of possible figures $F(R)$ also increases dramatically with the number of sites. Thus, a sensible selection of the figures, which are included in the CE, takes a crucial role if the prediction errors are to be limited to the smallest possible value. This selection is realized by a genetic algorithm (GA),[9] which optimizes the figures chosen for the CE. In order to calculate the predictive power of a CE, the resulting set of DFT input structures (in our case, the energies of the selected adsorption configurations were used as input structures) is divided into two subsets. One of them is a set of N structures out of the total number of calculated DFT structures N_{tot} reserved for testing the predictive power. The other subset contains $N_{\mathrm{tot}}-N$ structures used for the construction of the ECI. This scheme is repeated for n different construction sets with different input structures. The quality for the predictive power of a CE is then quantified by a fitness measure which compares the energies of the N structures predicted via CE with those retrieved from DFT calculations. As fitness measure for the GA, the so-called "leave-many-out" cross-validation score (CVS) (Refs. 9 and 10)

$$S_{\mathrm{CV}} = \sqrt{\frac{1}{nN}\sum_{n\ \mathrm{sets}}\sum_{\substack{N\ \mathrm{pred.}\\ \mathrm{per\ set}}} \left|\Delta H_f^{\mathrm{DFT}}(\sigma) - \Delta H_f^{\mathrm{CE}}(\sigma)\right|^2} \quad (3)$$

was chosen and calculated based on the prediction error for the enthalpy of formation of an adsorbate configuration σ with hydrogen concentration x_{H}:

$$\Delta H_f(\sigma) = E_{\mathrm{ads}}(\sigma) - x_{\mathrm{H}}E_{\mathrm{ads}}^{\mathrm{full}} - (1-x_{\mathrm{H}})E_{\mathrm{ads}}^{\mathrm{clean}} \quad (4)$$

using the total heat of adsorption of the clean $E_{\mathrm{ads}}^{\mathrm{clean}}$ and of the fully covered surface $E_{\mathrm{ads}}^{\mathrm{full}}$. A "leave-one-out" scheme ($N=1$) has been applied and checked against a "leave-many-out" procedure, where N was set to approximately 10% of the input structures used for the CE fit. This is a necessary precaution, which helps to reduce the risk of overfitting, to which leave-one-out schemes are always sensitive.

The DFT calculations, which are required as input for the cluster expansion, were performed using the projector augmented wave method[11,12] of the Vienna *ab-initio* simulation package (VASP).[13–16] The exchange correlation was treated within the generalized gradient approximation according to Perdew *et al.*[17] (PW91). Application of this functional to bulk iridium results in a lattice parameter $a_0=3.878$ Å and a bulk modulus $B_0=3.40$ Mbar, which are close to the experimental values [$a_0^{\mathrm{exp}}=3.839$ Å (Ref. 18) and $B_0^{\mathrm{exp}}=3.55$ Mbar (Ref. 19)]. The surface was modeled by repeated surface slabs of nine Ir layers of 17.5 Å thickness, onto which the hydrogen as well as the monatomic Ir chains reside. The slabs were separated by a vacuum equivalent to a thickness of five Ir layers (9.7 Å). Ten Ir atoms per layer were considered to form a (5×2) cell (marked by a white frame in Fig. 1) with two additional Ir atoms in the first layer to allow for the (5×1)-H reconstruction. In consequence, the H coverage could be investigated in steps of 0.1 monolayers (MLs). The slabs were asymmetric in the sense that hydrogen adsorption and multilayer relaxation were considered only on one side. On the other side all four Ir interlayer spacings were kept fixed at the bulk value ($d_b=1.94$ Å). The structural optimization was stopped when the forces computed had decreased below 0.02 eV/Å. For the determination of ground-state energies, Brillouin-zone sampling used a $(4\times10\times1)$ Monkhorst-Pack mesh[20] consisting of up to 20 irreducible k points, depending on the symmetry of the investigated structure. It should be mentioned that Eq. (4) neglects the vibrational ground-state energy of hydrogen. As shown in Table I, which gives both the heat of adsorptions with and without (in brackets) consideration of the zero-point correction, for the system under consideration this contribution changes the heat of adsorption up to about 10% but does *not* influence the energetic hierarchy between individual adsorption configurations. This is in agreement with our earlier investigations[21] for the hydrogen adsorption on the unreconstructed Ir(100) surface. Since in the present work the application of the methodical concept plays the most important role, we have neglected the vibrational contribution to the DFT input energies of the CE. Of course, this approximation has to be verified for any individual system.

TABLE I. Heat of adsorption E_{ads} in meV for single-site adsorption with and without (in brackets) the zero-point correction.

Bridge sites		Top sites		Hollow sites	
Site	E_{ads}	Site	E_{ads}	Site	E_{ads}
B1	**804 (848)**				
B2	**649 (690)**				
B3	**634 (675)**	T1	537 (574)		
B4	**611 (652)**	T2	519 (557)		
B5	444 (481)	T3	498 (536)	H1	304 (301)
B6	Instable	T4	Instable	H2	Instable

The ground state of the clean Ir(100) surface is the (5×1)-hex-reconstructed phase. For high enough temperatures (>180 K) hydrogen adsorption induces a transformation of the quasihexagonal surface to a phase characterized by atomic rows of monatomic width which reside on an unreconstructed (100)-(1×1)-like substrate.[1]Scanning tunneling microscopy images of the Ir(100)-(5×1)-H surface show that these rows are nearly regularly arranged with an average lateral spacing of $5a$ (with $a=2.715$ Å the atomic diameter and surface lattice parameter).

Within the Ir(100)-(5×1)-H surface there are 12 inequivalent adsorbate sites (six bridge, four top, and two hollow sites, Fig. 1). Table I shows that for single-site adsorption, the four bridge sites B1, B2, B3, and B4 (bold) are the most stable ones. Thereby, the highest heat of adsorption is found for occupation of the B1 site, i.e., the bridge site of the monatomic Ir chains. This certainly makes B1 at first to the

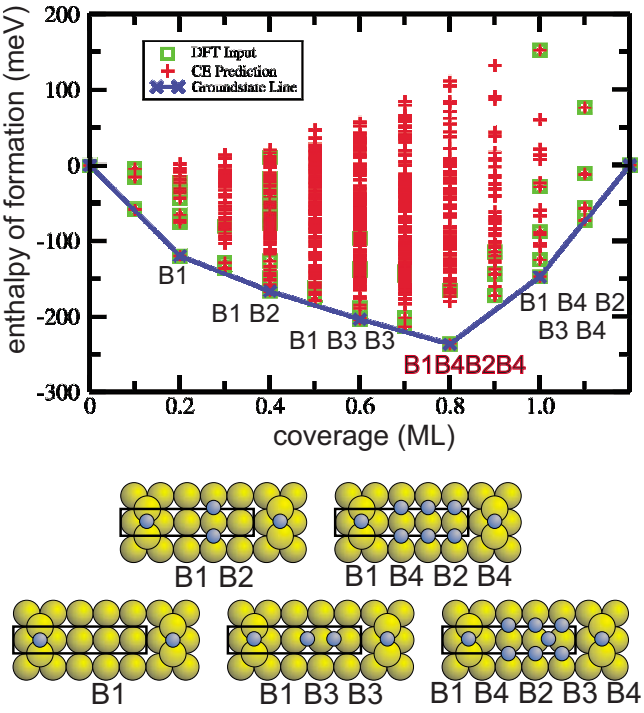

FIG. 2. (Color online) Ground-state diagram and corresponding ground-state configurations obtained for a ground-state search within a (5×2) unit cell on the Ir(100)-(5×1)-H surface.

preferred adsorption site of the hydrogen atoms. Further DFT calculations, which will be presented in a different paper, indicate that the occupation of any other site than B1, B2, B3, and B4 is unlikely for coverages up to 1.2 ML. This is supported by the fact that the lateral interaction between the individual hydrogen atoms result to be much weaker than the hydrogen-substrate interaction. Furthermore, temperature-programmed desorption measurements show that the saturation coverage is 0.8 ML.[22] For these reasons, we can safely limit our further ground-state search to configurations consisting exclusively of these four inequivalent bridge sites and still cover the full regime of experimentally observable coverages. Due to the symmetry of the (5×1)-H surface this results in a total of six possible adsorption sites, as the sites B3 and B4 both have symmetry equivalencies within the (5×1) unit cell.

There is, however, no argument for neglecting the interaction between hydrogen atoms *along* the rows so that an extension of the model system in this direction is necessary. We have therefore performed *a full ground-state search of all the configurations within a* (5×2) unit cell on the Ir(100)-(5×1)-H surface, which requires the calculation of 1124 symmetrically inequivalent adsorbate configurations. For full convergence of the ground-state diagram shown in Fig. 2, the calculation of 61 adsorbate configurations by DFT was necessary, using the resulting energies as input for the CE fitting scheme. The genetic algorithm was applied to a pool of 114 pair, triplet, and quadruple figures, which results in the choice of 40 figures. The resulting CVS calculated for this best-fit set of figures was 0.9 meV for the leave-out-one scheme and 1.3 meV when applying leave-out-many. The maximum deviation between DFT input energies used for the

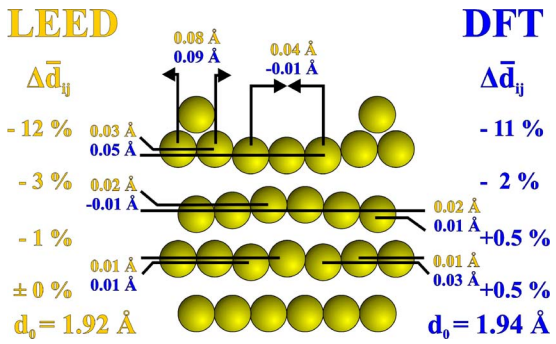

FIG. 3. (Color online) Comparison of structural parameters as determined by quantitative LEED (Ref. 1) and for the predicted B1B4B2B4 ground-state configuration.

construction of the ECI and CE energies is as low as 0.8 meV (1.2 meV for leave-out-many). So, the error due to the CE itself is thus completely negligible in comparison to the error of the DFT calculations on which it is based. It is important to notice that this high level of accuracy can only be obtained by including higher-order figures into the CE. A CE fit with pair figures only results in a much worse CVS (20 meV) and a maximum deviation of 9.5 meV between CE and DFT. At least for a CE of the present system, we can therefore state that the common assumption that pair interactions are sufficient to describe an adsorbate system is wrong.

The search finds five stable ground states between 0 and 1.2 ML coverage. Two of them mark especially pronounced kinks in the ground-state line and therefore deserve special attention. At $\theta=0.2$ ML the stable ground state is the single occupation of the site B1 on the Ir chains as could be anticipated from the energetics in Table I. At $\theta=0.8$ ML the stable ground state is the full occupation of the B1, B2, and both equivalent B4 sites (Fig. 2, configuration "B1B4B2B4"). The coverage of this ground state coincides with the saturation coverage and, therefore, the structure of this adsorbate configuration is easily accessible by low-energy electron diffraction (LEED) experiments. Even though hydrogen is almost completely invisible to LEED on strongly scattering substrate atoms as Ir, the substrate structure—i.e., the adsorbate-induced local relaxations of substrate atoms—does give clear evidence of the occupied adsorbate sites.[23,24] Comparing the substrate structure obtained by DFT for the ground-state adsorbate configuration determined by CE with the geometry determined by quantitative LEED (Ref. 1) yields very small deviations of at most 0.03 Å for all vertical and 0.05 Å for all lateral parameters. This lies well within the error bars for DFT-LEED comparisons. The detailed structural comparison is displayed in Fig. 3.

In summary, we have presented an approach for the determination of ground states for an arbitrary number of inequivalent sites. We believe that it will be of great use for complicated adsorbate systems where the occupation of several adsorbate sites makes an intuitive guess of the correct ground-state adsorbate configurations difficult—if not impossible—due to the huge configuration spaces involved with the number of adsorbate sites. Thereby, the CE method does not demand simplifications as the restriction to pair interactions which would be insufficient for the system under

consideration. Based on the energetics of geometrically fully relaxed structures, we have determined the ground-state line of the Ir(100)-(5×1)-H surface over the complete coverage range, which is experimentally observable. The ground state identified for saturation coverage could even be verified by a comparison of the resulting substrate structure to LEED experiments. We could furthermore show, that the CE can be employed without any further error than that of the *ab initio* input energetics, as long as the method is implemented in conjunction with state-of-the-art techniques such as the genetic algorithm.

*Corresponding author. FAX: +49-9131-8528400; stefan.mueller@physik.uni-erlangen.de

[1] L. Hammer, W. Meier, A. Klein, P. Landfried, A. Schmidt, and K. Heinz, Phys. Rev. Lett. **91**, 156101 (2003).
[2] A. Klein, A. Schmidt, L. Hammer, and K. Heinz, Europhys. Lett. **65**, 830 (2004).
[3] J. M. Sanchez, F. Ducastelle, and D. Gratias, Physica A **128**, 334 (1984).
[4] S. Müller, J. Phys.: Condens. Matter **15**, R1429 (2003).
[5] Y. Zhang, V. Blum, and K. Reuter, Phys. Rev. B **75**, 235406 (2007).
[6] M. H. F. Sluiter and Y. Kawazoe, Phys. Rev. B **68**, 085410 (2003).
[7] R. Drautz, H. Reichert, M. Fähnle, H. Dosch, and J. M. Sanchez, Phys. Rev. Lett. **87**, 236102 (2001).
[8] S. Müller, M. Stöhr, and O. Wieckhorst, Appl. Phys. A: Mater. Sci. Process. **82**, 415 (2006).
[9] G. L. W. Hart, V. Blum, J. Walorski, and A. Zunger, Nat. Mater. **4**, 391 (2005).
[10] K. Baumann, Trends Analyt. Chem. **22**, 395 (2003).
[11] P. E. Blöchl, Phys. Rev. B **50**, 17953 (1994).
[12] G. Kresse and D. Joubert, Phys. Rev. B **59**, 1758 (1999).
[13] G. Kresse and J. Hafner, Phys. Rev. B **47**, 558 (1993).
[14] G. Kresse and J. Hafner, J. Phys.: Condens. Matter **6**, 8245 (1994).
[15] G. Kresse and J. Furthmüller, Phys. Rev. B **54**, 11169 (1996).
[16] G. Kresse and J. Furthmüller, Comput. Mater. Sci. **6**, 15 (1996).
[17] J. P. Perdew, J. A. Chevary, S. H. Vosko, K. A. Jackson, M. R. Pederson, D. J. Singh, and C. Fiolhais, Phys. Rev. B **46**, 6671 (1992).
[18] D. E. Gray, *American Institute of Physics Handbook*, 7th ed. (McGraw-Hill, New York, 1972).
[19] C. Kittel, *Introduction to Solid State Physics*, 7th ed. (Wiley, New York, 1996).
[20] H. J. Monkhorst and J. D. Pack, Phys. Rev. B **13**, 5188 (1976).
[21] D. Lerch, A. Klein, A. Schmidt, S. Müller, L. Hammer, K. Heinz, and M. Weinert, Phys. Rev. B **73**, 075430 (2006).
[22] A. Klein, PhD thesis, University Erlangen-Nürnberg, 2007.
[23] D. Lerch, S. Müller, L. Hammer, and K. Heinz, Phys. Rev. B **74**, 075426 (2006).
[24] H. C. Poon, D. K. Saldin, D. Lerch, W. Meier, A. Schmidt, A. Klein, S. Müller, L. Hammer, and K. Heinz, Phys. Rev. B **74**, 125413 (2006).